Available online at www.elixirpublishers.com (Elixir International Journal)

Thermal Engineering

Elixir Thermal Engg. 56A (2013) 13715-13718

ISSN: 2229-712X

Prediction of bubble lift-off diameter in subcooled flow boiling using AVL fire

Reza Hemmat Khanlou, Arash Mohammadi and Sayed Ali Jazayeri
K.N.Toosi University of Technology, Pardis Ave.,Molasadra St, Tehran, Iran.

ARTICLE INFO

Article history:
Received: 10 August 2012;
Received in revised form:
21 March 2013;
Accepted: 23 March 2013;

Keywords
Heat transfer,
Subcooled flow boiling,
Bubble lift-off.

ABSTRACT

Subcooled nucleate flow boiling is a very efficient heat transfer mechanism and therefore applied in many technical applications. A numerical simulation was conducted to predict the bubble lift-off size in a BWR-scaled vertical upward annular channel, which had been compared with some experimental results. A force balance analysis of a growing bubble was performed to predict the bubble lift-off size.

Introduction

Since nucleate boiling heat transfer occurs frequently in various industrial applications, fundamental knowledge of bubble growth, departure and lift-off from heated surface is important. Better knowledge may help to improve efficiency and reliability of boiling process. Bubble behavior in subcooled flow boiling was studied by many researchers. In early work by Gunther [1], it was observed that bubbles grew and collapsed while sliding along the heated wall under the influence of bulk flow. In the experiments by Bibeau and Salcudean [2], bubbles slide along the heated surface before being ejected into the subcooled bulk liquid. Since the bubbles are collapsed due to condensation, they did not travel far downstream after nucleation. Zeitoun and Shoukri [3] also observed that the bubbles tended to be detached from the heated wall. They developed an empirical correlation for the mean bubble diameter as a function of Reynolds number, Jakob number and the boiling number. Situ et al. [4,5] carried out forced convection subcooled water boiling experiments using a vertical annular channel as the test section. They measured the bubble lift-off diameter for several different working conditions. Based on Situ et al. [5] experiments, theoretical discussions are made in the present article to predict bubble lift-off size using AVL Fire CFD software.

Mathematical Formulation

Prediction of bubble behavior in forced convective subcooled boiling flow is of considerable interest to boiling water reactor (BWR) safety. According to the hypothesis of Zeng and his coworkers, the whole process of the bubble detachment basically evolves in three different stages, as schematically shown in Fig. 1.

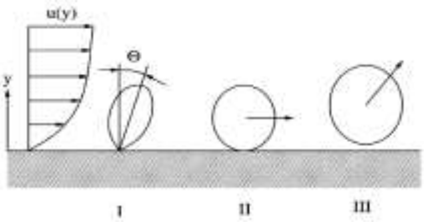

Fig. 1Three stages of a vapor bubble departing from the heater surface

Tele:
E-mail addresses: Reza_hemmatkhanlou@sina.kntu.ac.ir

At the first stage the bubble is attached to its nucleation site, and it is inclined by the angle θ ought to the hydrodynamic flow forces. The attached bubble is growing until it reaches a critical departure volume, where the bubble is dragged off its nucleation site. After the departure stage begins the bubble slides in upright posture ($\theta = 0$) along the heated wall. It keeps growing in size until it reaches a bubble volume, where the buoyancy force is sufficiently high to make the bubble lift off from the wall, which marks the beginning of the stage III.

Figure 2 shows the forces acting on a bubble at its nucleation site (some other forces exist but they are negligible). These forces are:

- The growth force F_{du}: the growth force is also called unsteady drag force.

$$F_{du} = -\rho_f(T_{sat})4b^4Ja^4\left(\frac{\lambda}{\rho_f c_p}\right)^2\frac{1}{\pi}\left(\frac{3}{2}C_s - 1\right) \quad (1)$$

Where the Jakob number is defined as:

$$Ja = \frac{\rho_f c_{pf}\Delta T_{sat}}{\rho_g i_{fg}} = \frac{\rho_f c_{pf}(T_w - T_{sat})}{\rho_g i_{fg}} \quad (2)$$

Where c_{pf}, ΔT_{sat}, i_{fg}, T_w and T_{sat} are, respectively, the specific heat of liquid at constant pressure, the wall superheat, the latent heat, the wall temperature, and the saturation temperature. C_s also accounts for the non-sphericity of the bubble and for the presence of the wall.

- The buoyancy and gravity forces F_p and F_g: the pressure force (buoyancy force) on a bubble by the surrounding liquid is expressed as

$$F_p = \rho_f g V_b \quad (3)$$

Where V_b is the bubble volume. The gravity force can be obtained by

$$F_g = -\rho_g g V_b \quad (4)$$

• The quasi-steady drag force F_{qs}: for the quasi-steady drag force, Klausner et al. [6] modified the expression by Mei and Klausner [7] by taking into account the effect of the wall as

$$F_{qs} = 6\pi\rho_f(T_{sat})\frac{\mu_f}{\rho_f}u_r r[\frac{2}{3}[(\frac{12}{Re_b})^m + 0.796^m]^{-\frac{1}{m}}] \quad (5)$$

Where u_r is the velocity at the bubble center and Re_b is the bubble reference Reynolds number. The bubble velocity is assumed as equal as u_f (i.e. liquid phase velocity) when the bubble is not sliding, and it is zero when the bubble velocity is the same as the liquid velocity. Bubble Reynolds number Re_b is calculated from the following equation

$$Re_b = \frac{2r_b u_r}{v_f} \quad (6)$$

Where r_b is the bubble radius.

• The shear lift force F_{sl}: Saffman [8] derived the shear lift force on a solid sphere at low Reynolds number. Auton [9] derived an expression for the shear lift force on a sphere in an inviscid shear flow. Mei and Klausner [10] modified Saffman's model to suit for a bubble, and interpolated with Auton's equation to derive an expression for shear lift force over wide range of Reynolds number as

$$F_{sl} = \frac{1}{2}C_l\rho_f\pi r_b^2 u_r^2 \quad (7)$$

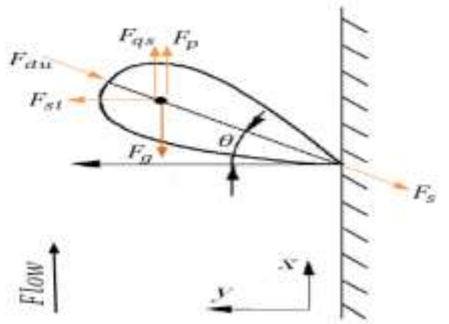

Fig.2 Forces applied on a bubble in its nucleation site

Where u_r is the relative velocity between the bubble center of mass and the liquid phase, i.e., $u_r = u_f - u_g$, and the C_l is the shear lift coefficient given by [6].

$$C_l = 3.877G_s^{1/2}(Re_b^{-2} + 0.014G_s^2)^{1/4} \quad (8)$$

Where G_s is the shear rate.

When the bubble starts to slide on the wall, it is assumed that its velocity is the same as the liquid around. Therefore the bubble velocity u_r and the velocity gradient in the shear rate G_s are estimated due to Reichart law of the wall. The departure diameter is then calculated as the root of the force balance in x-direction.

When the bubble lifts-off the bubble main axis is vertical ($\theta = 0$) and so is its motion. The force balance in the y-direction at the moment of lift-off is shown in Fig. 3. the bubble surface tension may be neglected at the bubble lift-off because the bubble contact area on the heated wall becomes zero at the moment of lift-off. The unsteady drag force becomes normal to the flow direction. Then the force balance in the y-direction results in

$$F_{du} + F_{sl} = 0 \quad (9)$$

Substituting the expressions of the unsteady-drag force and shear lift force into above equation and solving the equation yields the lift-off diameter.

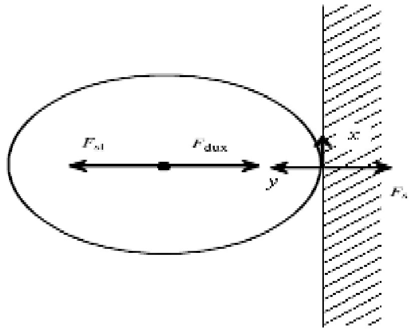

Fig.3 Force balance of a vapor bubble at lift-off

Experimental description

To validate the AVL Fire CFD software with the bubble lift-off model, the experimental data of subcooled boiling tests were utilized [5]. In the experiment, the subcooled boiling phenomena in a vertical annulus channel were observed in subcooled boiling facility shown in Fig. 4. The inner diameter of the test section is 38.1 mm and the outer diameter of the heater rod is 19.1 mm. the heater rod consists of three parts. The first part is an unheated section (212 mm in length) to regulate the water condition at the inlet, the second part is a heated section (1730 mm in length) for the simulation of nucleate boiling and the third part is an unheated section (728 mm in length) for the bubble condensation at the top region. The test section is made of translucent glass for the purpose of image capturing. Boiling experiment in subcooled flow with a constant rate of subcooling and under atmospheric pressure conditions were carried out. The boiling process was visualized by a high-speed video technique. The subcooled water is held in the main tank. The main tank has a cartridge heater and heat exchanger to control the test-section inlet subcooling.

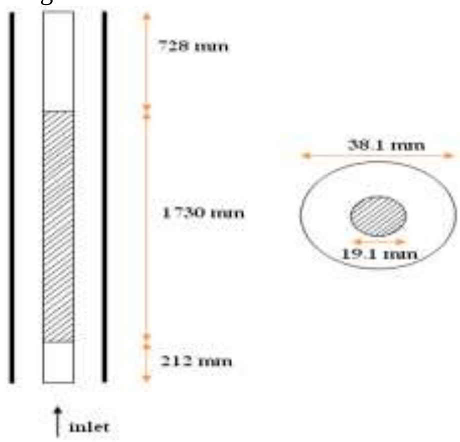

Fig.4 Test section of BWR facility

In order to capture the very short bubble growth period, i.e., only a few milliseconds, a CCD camera with resolution of 80×120 pixels was focused in desired nucleation sites in the distance of z_d from the BWR inlet. And a Matlab program has been developed to analyze the digital images and to calculate the bubble diameter. The inlet temperature was measured by the thermistor probe and a pressure transducer was used to record the pressure drop across the test section.

Comparison of model predictions with experiments

Situ et al. [5] investigated 91 experimental conditions and measured bubble lift-off diameter in different distances (z_d) from the BWR inlet. Five groups of data from test series were selected for the validations are summarized in table 1.

Table 1 Summary of data test used for validation

Groups No.	Inlet Velocity (m/s)	Wall heat flux (kW/m^2)	z_d Distance from the inlet (m)
1	0.923	144	0.700
2	0.752	143	0.631
3	0.749	103	0.640
4	0.515	102	0.626
5	0.502	62.5	0.668

To simulate the BWR in AVL Fire software, a 3d mesh is generated as illustrated in Fig. 5.

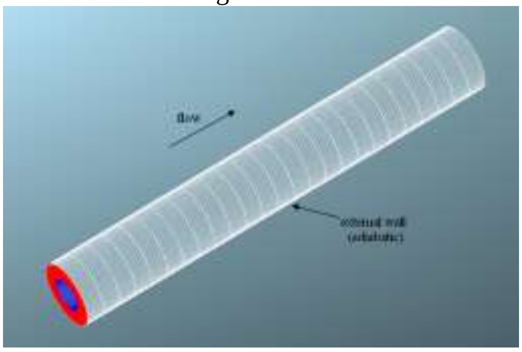

a)

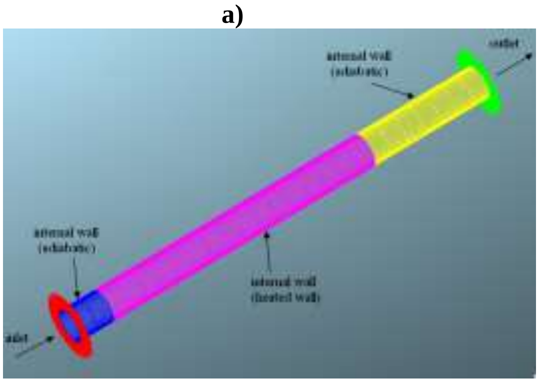

b)

Fig.5 CFD annulus mesh

For each data point, the inlet fluid temperature and inlet bulk velocity in the CFD simulation were specified according to the test conditions. On the heated wall a constant heat flux condition was applied. The rest of the walls were assumed to be adiabatic. Figure 6 (a-e) shows the comparison of measured bubble lift-off diameter in different distances from the inlet versus inlet temperature under different wall heat fluxes.

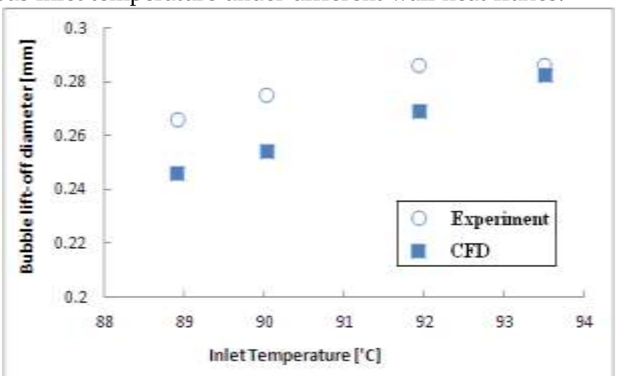

a) group 1

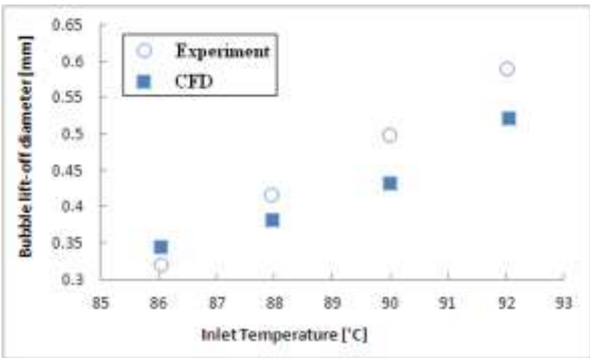

b)group 2

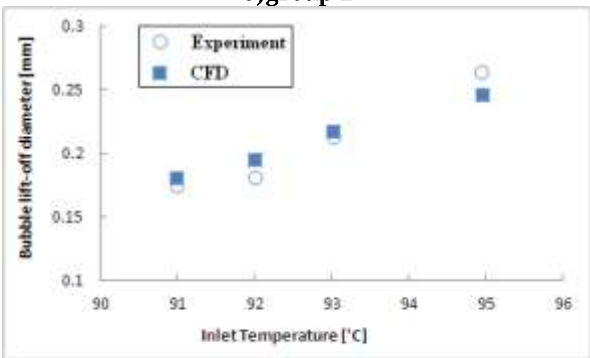

a) group 3

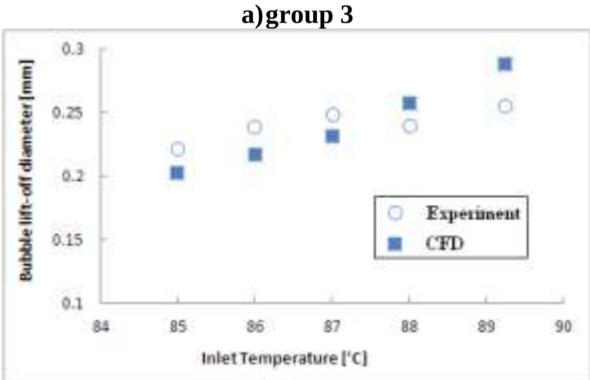

d) **group 4**

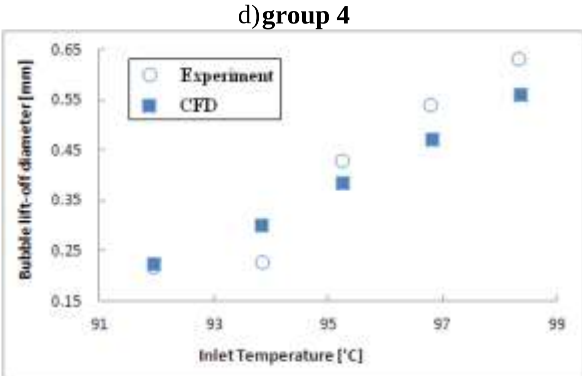

e) group 5

Fig.6 Comparison of CFD and experimental results of groups 1-5

Fig. 5 (a-e) show the measured and predicted bubble lift-off diameters against the inlet temperature. The figures indicate that the bubble lift-off diameter increases as the inlet temperature increases. The predictive results agree well with the experimental data and imply a linear behavior with increasing the inlet temperature. Because nucleation sites are captured at different axial positions, and have different cavity sizes, it is rather difficult to capture the bubble lift-off diameter between the nucleation sites.

Conclusion

Forced subcooled flow boiling experiments were conducted in a BWR vertical upward annular channel by using water as working fluid. The experiments were performed at atmosphere pressure. The inlet temperature ranged from 80.0 to 98.5'C; the inlet velocity varied from 0.487 to 0.939 m/s. A high-speed digital camera was utilized to capture images of growing bubble in specific distances from the inlet. The images were then analyzed via Matlab image processing developed codes. To predict the bubble lift-off diameter, a 3d mesh was generated in AVL Fire software and was run according to experiments operating conditions. The CFD results are in good satisfactory with experimental data. Results indicate that bubble lift-off diameter increases with increasing the inlet temperature.

Nomenclature

model constant [-]
specific heat at constant pressure [J/]
constant [-]
diameter [m]
hydraulic diameter [m]
force [ ]
gravitational acceleration [r]
shear lift coefficient [-]
latent heat [ ]
jakob number[-]
constant [-]
pressure [N]
prandtl number [-]
radius [m]
Reynolds number [-]
temperature [ ]
velocity [ ]
axial coordinate [m]
wall normal coordinate [m]
distance from the inlet [m]

Greek symbols

μ dynamic viscosity[kg]
mass density [kg]
conductivity [W/mK]
surface tension [k]
inclination angle [ ]

Subscripts

bulk
bubble
bubble growth
liquid phase
vapor phase
constant pressure
quasi steady
saturated
shear lift
wall

References

[1] F.C. Gunther, photographic study of surface-boiling heat transfer to water with force convection, J. Heat Transfer 73 (1951) 115–123.
[2] E.L. Bibeau, M. Salcudean, A study of bubble ebullition in forced-convective subcooled nucleate boiling at low pressures, Int. J. Heat Mass Transfer 37 (1994) 2245–2259.
[3] O. Zeitoun, M. Shoukri, Bubble behavior and mean diameter in subcooled flow boiling, J. Heat Transfer 118 (1996) 110–116.
[4] R. Situ, Y. Mi, M. Ishii, M. Mori, Photographic study of bubble behaviors in forced convection subcooled boiling, Int. J. Heat Mass Transfer 47 (2004) 3659–3667.
[5] R. Situ, T. Hibiki, M. Ishii, M. Mori, Bubble lift-off size in forced convective subcooled boiling flow, Int. J. Heat Mass Transfer 48 (2005) 5536–5548.
[6] Klausner, J.F., Mei, R., Bernhard, M., Zeng, L.Z., 1993. Vapor bubble departure in forced convection boiling. Int. J. Heat Mass Transfer 36, 651–662.
[7] R. Mei, J.F. Klausner, Unsteady force on a spherical bubble at finite Reynolds number with small fluctuations in the free-streamvelocity, Phys. Fluids A 4 (1992) 63–70.
[8] P.G. Saffman, The lift on a small sphere in a slow shear flow, J. Fluid Mech. 22 (1965) 385–400.
[9] T.R. Auton, The lift force on a spherical body in a rotational flow, J. Fluid Mech. 183 (1987) 199–218.
[10] R. Mei, J.F. Klausner, Shear lift force on spherical bubbles, Int. J. Heat Fluid Flow 15 (1994) 62–65.